J. Fluid Mech. (1982), *vol.* 125, *pp.* 359–373
Printed in Great Britain

Oscillatory flows at intermediate Strouhal number in asymmetric channels

By IAN J. SOBEY
School of Mathematics, University of Bristol, U.K.

(Received 4 May 1982)

We consider separated oscillatory flows in asymmetric channels when the Strouhal number is sufficiently great for the flow not to be quasi-steady, but where the flow is not dominated by viscous effects. In this range, we show that numerical calculations predict the expansion of vortices during a deceleration and we investigate these flows in several different geometries. These calculations are supported by experimental observations of the motion of small particles immersed in water.

1. Introduction

In this paper we present the results of observations and calculations of oscillatory flows in asymmetric channels at intermediate Strouhal numbers. We are concerned with flows in channels in which the geometry imposes such pressure gradients on the fluid that separation is the ultimate outcome. Flow under these conditions in a symmetric channel has been described by Sobey (1980) and Stephanoff, Sobey & Bellhouse (1980), hereafter referred to as I and II. Here we shall see if asymmetries in the channels modify the conclusions of those papers.

In a channel of minimum gap $2h$ with a flux $2hU$ of fluid of viscosity ν, the single most important parameter that characterizes the flow is the Reynolds number

$$R = \frac{hU}{\nu}.$$

If the flow is unsteady, with frequency Ω and peak flux $2hU$, another parameter occurs, the Strouhal number

$$S = \frac{h\Omega}{U}.$$

One of the main conclusions of I concerned the importance of observing that in oscillatory flow both these parameters are equally important. If the Strouhal number is large, $O(1)$, then viscosity dominates the flow and inertial separation never occurs, regardless of the size of the Reynolds number. If the Strouhal number is $O(10^{-4})$ then a true quasi-steady flow exists, as described by Sobey (1982). Between these orders there is an intermediate range in which inertial separation occurs but the flow does not behave in a quasi-steady fashion. In a symmetrical channel it is observed that there is a critical Reynolds number that must be exceeded in order for separation to occur. For Reynolds numbers below the critical value the flow is dominated by viscosity. The critical Reynolds number is a function of channel geometry, and increases weakly with Strouhal number in the range we are considering. For very small Strouhal numbers the critical value is the same value at which a steady flow separates, as indicated by describing that region as quasi-steady. It should also be noted that a second and larger critical Reynolds number will exist at which the flow will cease to be laminar and become turbulent.

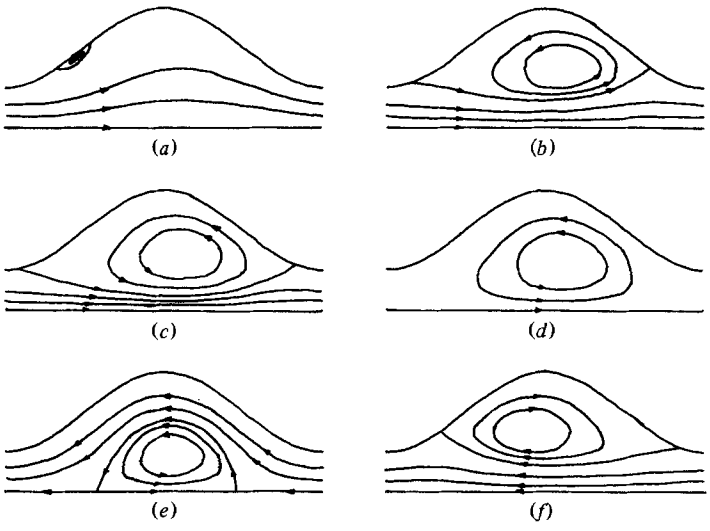

FIGURE 1. Calculated streamlines in the upper half of a symmetric channel; $R = 75$, $S = 0{\cdot}01$, $L = 8$, $D = 2$. (*a*) $t = 0{\cdot}1$; (*b*) 0·25; (*c*) 0·45; (*d*) 0·5; (*e*) 0·55; (*f*) 0·75.

If the critical Reynolds number is exceeded then separation occurs during acceleration of the flow. This situation is illustrated in figure 1 for flow in a symmetrical furrowed channel. Initially the flow is subjected to a pressure gradient in the direction of the flow because of the acceleration. This causes the fluid to stream through the channel without separating. The channel geometry will impose a pressure gradient opposing the direction of flow in the region of increasing channel width. The magnitude of this adverse pressure gradient will increase as the flow magnitude increases, while the pressure gradient driving the flow will decrease as the time of peak flow approaches. Eventually the adverse pressure gradient will exceed the pressure gradient driving the flow and shortly after this the flow may separate (figure 1*a*). Note that as we are discussing Reynolds numbers that exceed the critical value we are assuming that separation does in fact happen. Once separation occurs a vortex forms and grows rapidly, until at peak flow there may be a considerable region of recirculating flow (figure 1*b*). It is during the deceleration that the vortices behave in a remarkable manner. As the flow magnitude decreases, the vortices do not decrease in size, as happens in quasi-steady flow, but expand, gradually bulging into the mainstream (figure 1*c*). As the flux of fluid through the channel vanishes, the vortices remain spinning in the fluid, and they effectively occupy the entire channel (figure 1*d*). This behaviour is possibly not surprising because although the Reynolds number may be large we are dealing with a viscous fluid, and continuity of stress should ensure that moving fluid entrains stationary fluid before the whole fluid would come to rest. Indeed flow during deceleration is subjected to a general adverse pressure gradient tending to accelerate any existing region of reverse flow. If the flux of fluid now becomes negative then near the walls the fluid is already flowing backwards and the mainstream passes between the vortex and the walls, ejecting the vortex from the furrow (figure 1*e*). Eventually the ejected vortex is entrained into the mainstream by viscous action, and the separation process repeats itself, a new counter-rotating vortex forming in the furrow (figure 1*f*). The process of vortex ejection and entrainment occurs very rapidly at the time of reversal of the fluid flux.

Our main concern here is the effect on the flow patterns we have described above of asymmetries in the channel geometry. The process of vortex formation and ejection is a powerful source of convective mixing, and devices that utilize this process may suffer from imperfect manufacture, such as misaligned channel walls, so it is important to know if poor alignment would substantially alter the structure of the flow cycle. Indeed it might be thought that deliberate introduction of asymmetries would augment the vortex-mixing process. In addition, the asymptotic work of Smith (1976) predicts that in steady flow through an asymmetric channel the mainstream will follow the mean displacement of the walls, a conclusion that is supported by the calculations and observations we present.

In dealing with the effect of small channel asymmetries there are guidelines we would expect to be followed. If a flow in a symmetric channel separates at a particular Reynolds number, then at the same Reynolds number an asymmetry would inhibit separation if the rate of increase of channel width in the flow direction was decreased. This would lower the adverse pressure gradient due to changing cross-section while the forward pressure gradient driving the main flux of fluid would be largely unaltered. Conversely, an asymmetry that increased the rate of channel expansion would reduce the Reynolds number at which separation occurred.

We have used both numerical and experimental methods to study flows in asymmetric channels. In §2 we describe the mathematical problem and discuss details of the numerical solution, and in §3 we describe the experiments. In §4 we study flow through a channel with sinusoidal wall variations where two walls can be misaligned by some angle ϕ, where $0 \leqslant \phi \leqslant \pi$. In §5 we look at a few other interesting geometries, and finally in §6 we present our conclusions.

2. Mathematical formulation

Let $\hat{x}$ and $\hat{y}$ be a two-dimensional Cartesian coordinate system, and consider a channel of infinite extent whose boundaries are given by

$$\hat{y} = hf\left(\frac{\hat{x}}{h}\right), \quad \hat{y} = -hg\left(\frac{\hat{x}}{h}\right),$$

where f and g are twice-differentiable functions with period L, so that $f(x+L) = f(x)$ and $g(x+L) = g(x)$ (see figure 2). A fluid of kinematic viscosity ν flows through the channel with flux $\hat{Q}$, where

$$\hat{Q}(\hat{t}) = 2hU \sin 2\pi\Omega\hat{t},$$

and $\hat{t}$ is the time. If $\hat{u}$ and $\hat{v}$ are the velocities in the $\hat{x}$- and $\hat{y}$-directions respectively, we denote non-dimensional coordinates by

$$x = \frac{\hat{x}}{h}, \quad z = \frac{2(\hat{y}+hg)}{hf+hg}, \quad t = \Omega\hat{t},$$

so that the boundaries become $z = 0$ and $z = 2$. We define a stream function ψ by

$$\hat{u} = Up_1(x)\frac{\partial\psi}{\partial z}, \quad \hat{v} = -U\left[\frac{\partial\psi}{\partial x} + p_2(x,z)\frac{\partial\psi}{\partial z}\right],$$

where

$$p_1(x) = \frac{2}{f(x)+g(x)}, \quad p_2(x,z) = \frac{2g'-(f'+g')z}{f+g}.$$

This simple transform 'straightens' the walls, but of course will only provide the basis

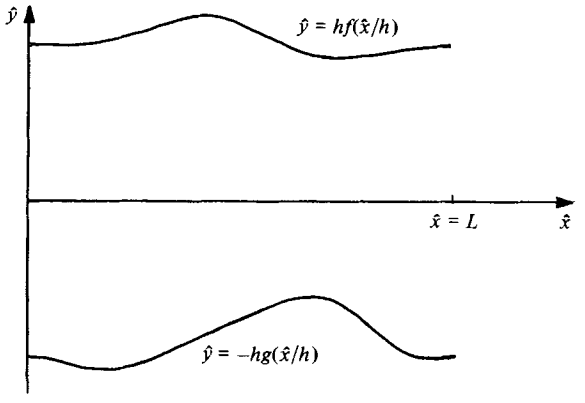

FIGURE 2. Schematic description of an asymmetric channel.

of a suitable numerical scheme if the walls are smooth, hence the requirement that f and g are twice-differentiable. In the cases we deal with here f and g are of sinusoidal variation and so this transformation is extremely useful.

In the transformed coordinates (x, z), Laplace's operator ∇^2 becomes

$$\nabla^2 = \frac{\partial^2}{\partial x^2} + \left(\frac{\partial p_2}{\partial x} + p_2 \frac{\partial p_2}{\partial z}\right) \frac{\partial}{\partial z} + 2p_2 \frac{\partial^2}{\partial x \partial z} + (p_2^2 + p_1^2) \frac{\partial^2}{\partial z^2}.$$

Then we can define the vorticity ω by

$$\omega = -\nabla^2 \psi,$$

and the vorticity-transport equation is

$$S \frac{\partial \omega}{\partial t} + \frac{\partial}{\partial x}(u\omega) + p_2 \frac{\partial}{\partial z}(u\omega) + p_1 \frac{\partial}{\partial z}(v\omega) = \frac{1}{R} \nabla^2 \omega,$$

where u and v are the non-dimensional velocities $\hat{u}/U$ and $\hat{v}/U$ respectively.

The boundary conditions are then

$$\psi|_{z=0} = 0, \quad \psi|_{z=2} = \sin 2\pi t,$$
$$\psi_z = 0 \quad \text{on} \quad z = 0 \quad \text{and} \quad z = 2.$$

We define the vortex strength $\Delta\psi$ to be the maximum value of $|\psi|$ minus the value of $|\psi|$ on the wall of the channel at that time. We have solved these equations numerically using a finite-difference scheme. Near $z = 0$ and $z = 2$ we used a fine mesh, while in the centre of the channel a coarse mesh was used. The vorticity-transport equation was solved using upwind differencing and a Dufort–Frankel substitution. The computational region was $0 \leqslant z \leqslant 2$ and $0 \leqslant x \leqslant L$, and the periodic nature of the walls allowed the solution to be iterated until the boundary conditions

$$\psi|_{x=0} = \psi|_{x=L}, \quad \omega|_{x=0} = \omega|_{x=L}$$

were satisfied. These particular boundary conditions represent an enormous simplification of the numerical problem, as it is not necessary to use approximate boundary conditions at upstream and downstream boundaries of the computational region. Further detail of the numerical solution are presented in Sobey (1980).

3. Experimental details

We have photographed flow patterns in asymmetric channels using the same methods as in II. A variable-speed motor drives a piston via a swash plate of adjustable stroke, and small channels machined from Perspex were attached to the piston unit. A slide projector was used as a simple light source. Small crystals of guanine (Merlmaid AA, The Mearl Corp., N.Y.) were used to visualize the flow. Such crystals are very small, about 10 μm, and have extremely high reflectivity. They are almost neutrally buoyant, settling out of water in a few hours, while a typical experiment would last a few minutes. The channels used had a half gap of 1 mm and the furrows were 4 mm long. Still photographs were taken using Kodak 2475 Recording film and an exposure time of $\frac{1}{60}$ s at $f/5{\cdot}8$. The photographs shown in figures 4 and 9 are meant to give a qualitative idea of the flow patterns, and are not a great deal of use in quantitative studies.

4. Channels with sinusoidal walls

Here we shall restrict our attention to the case

$$f(x) = 1+\tfrac{1}{2}D\left(1+\cos\frac{2\pi x}{L}\right),$$

$$g(x) = 1+\tfrac{1}{2}D\left(1+\cos\left(\frac{2\pi x}{L}+\phi\right)\right),$$

where ϕ represents the angle by which the two walls of the channel have been misaligned, either accidentally or deliberately. We shall refer to the walls $\hat{y} = hf$ and $\hat{y} = hg$ as the upper and lower walls respectively. One of the main contentions of I was that during a deceleration a vortex would not die away but rather grow until it filled the channel as well as the furrow in which it originated. We have described this process for a symmetrical channel in §1, and it is illustrated in figure 1. Here we discuss how the process of vortex formation and expansion is affected by offset channels of the type we are considering. To this end consider first the case $\phi = \pi$, where the channels are offset by exactly half a period and thus form a sinuous channel. Typical calculated flow patterns for this type of geometry are shown in figure 3 and photographs of particle motions that support the calculations are shown in figure 4. Early in the acceleration the fluid streams through the channel, with the flow direction mainly parallel to the walls. In this particular case the channel width remains constant, and so there can be no adverse pressure gradient due to changes in the channel width, although the pressure gradient required to make the fluid follow a sinuous path will have a component along the wall that opposes the fluid motion, and eventually separation occurs in the lee of the wall crests (figures 3*a*, 4*a*). When the flow decelerates, the vortices continue to grow in size, although it is apparent that the channel geometry has had a rather severe effect on the shape of the vortices (figures 3*b*, 4*b*). When the flux of fluid through the channel has almost vanished, the vortices expand to fill the channel and the centres of the vortices move upstream a short distance (figure 3*c*). Main-flow reversal now produces a most singular effect. As explained in I, an effect of vortex expansion is to leave residual motion, and this gives the fluid a preferred direction of motion when the main flow reverses direction. In a symmetric channel this effect resulted in the ejection of the vortices from the furrows and their being trapped in the centre of the channel as the main flow moved between the vortices and the walls. Here flow reversal still results in fluid moving around each

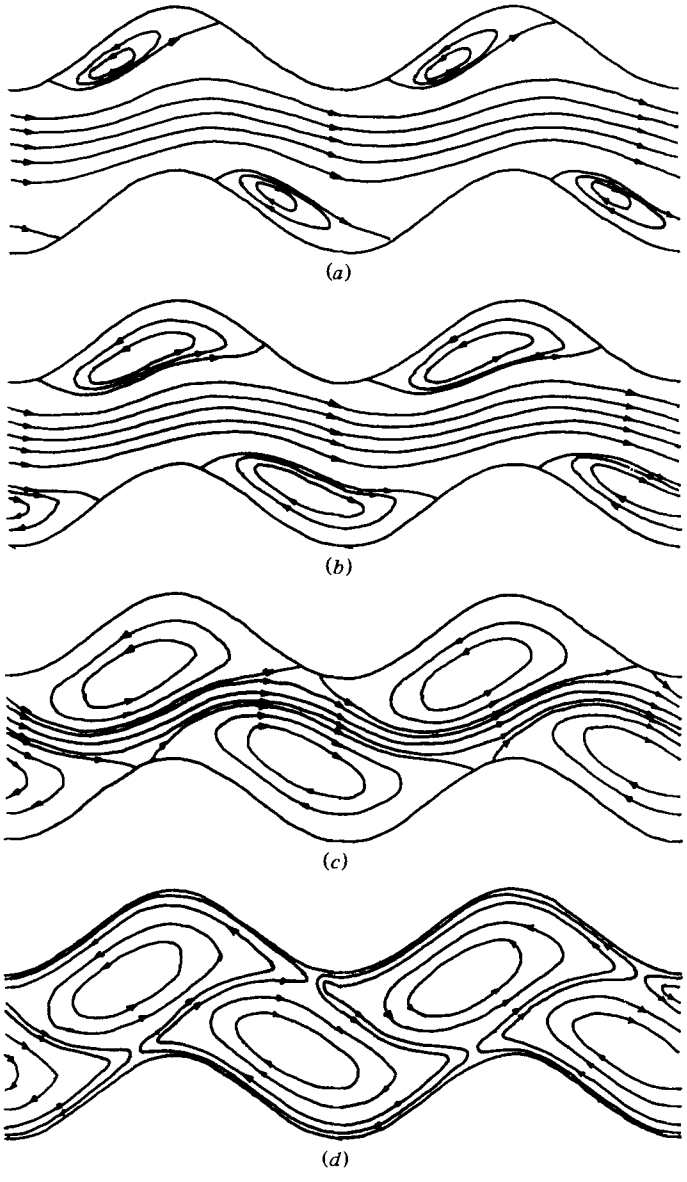

FIGURE 3. Calculated streamlines in a sinuous channel; $R = 50$, $S = 0{\cdot}01$, $L = 8$, $D = 2$. (a) $t = 0{\cdot}25$; (b) 0·40; (c) 0·49; (d) 0·502.

vortex, but now the vortices no longer appear in pairs adjacent to each other, but rather as a string along the channel. This means that the main flow must initially follow a highly convoluted path (figures $3d$, $4d$). The main flow then rapidly entrains fluid from the vortices, reducing their size until they disappear. The cycle of vortex formation, expansion, ejection and entrainment then continues as the flux of fluid through the channel oscillates.

Next we consider channels with a phase shift ϕ lying between 0 (described by figure 1) and π (described by figure 3). As ϕ varies we would expect to observe several different effects. Firstly there will be a difference between the strength of the

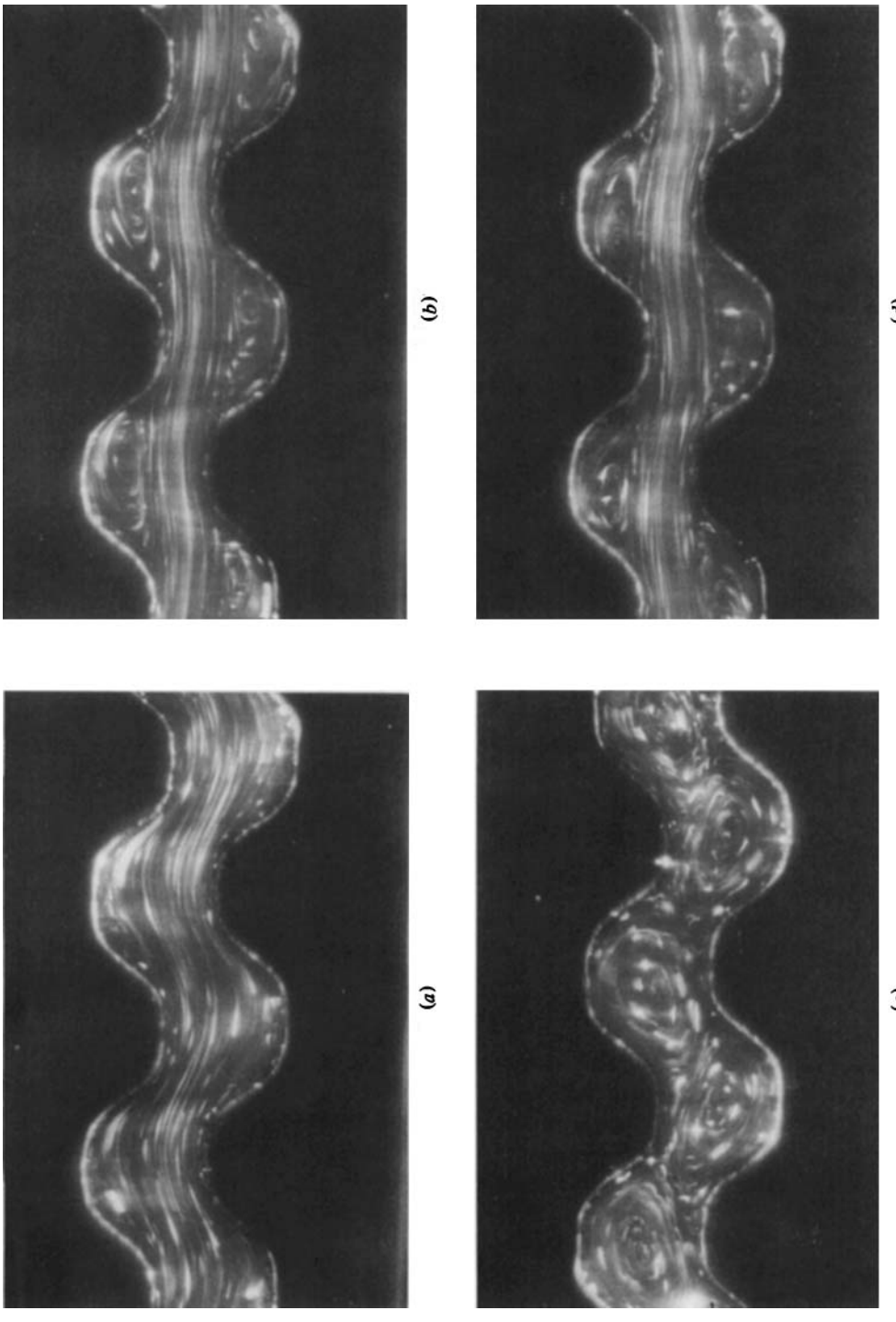

FIGURE 4. Oscillatory flow in a sinuous channel; $h = 1$ mm, $Lh = 4$ mm, $R = 100$, $S = 0{\cdot}006$ flow initially from left to right. (*a*) Early in the acceleration; (*b*) near peak flow, (*c*) main flow at rest; (*d*) peak flow from right to left.

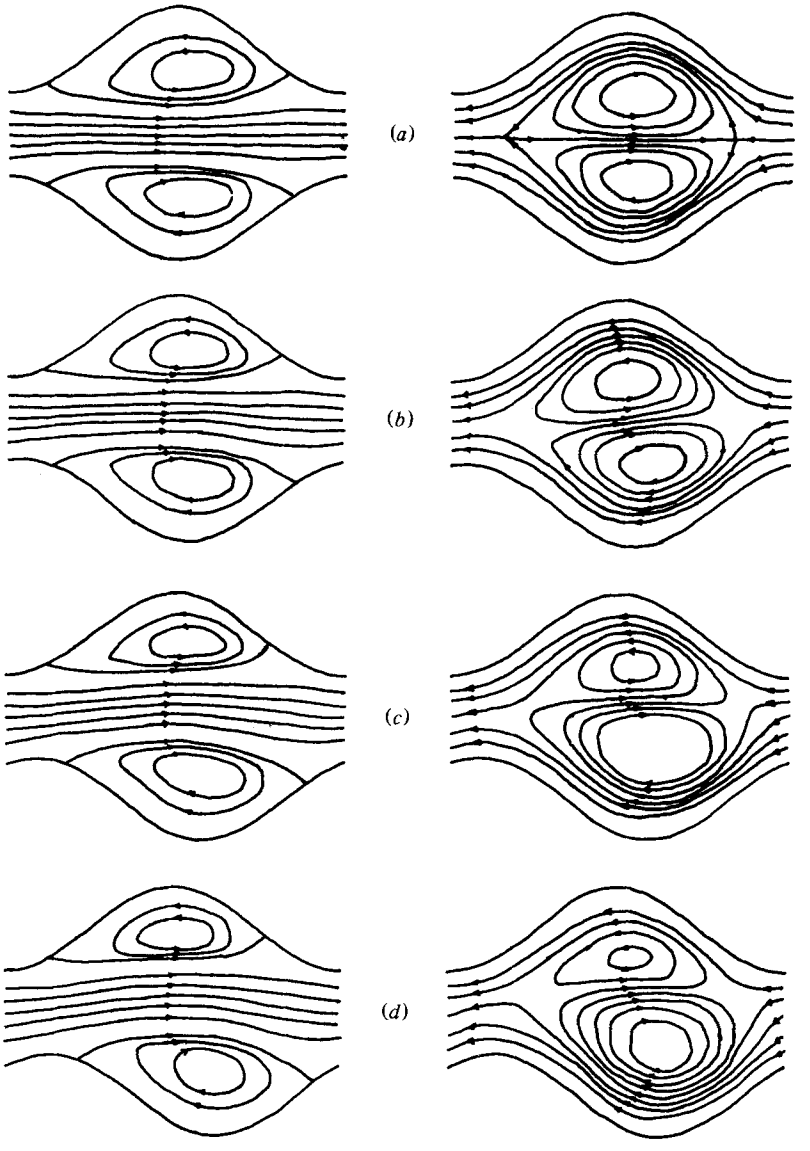

FIGURE 5(*a–d*). For caption see facing page.

vortices that form on the upper and lower walls. Secondly, during any expansion of the vortices there will be an interaction between vortices of different sizes and strengths. Finally, there is the question of how the vortices react to reversal of the main flow. In figure 5 we show the effect of varying ϕ on the instantaneous streamlines for eight values of ϕ and at two times, peak flow and just after reversal of the main flow. In the case of a symmetric channel (figure 5*a*), at peak flow the vortices fill the furrows with the vortex centres located just downstream of the furrow apex. As the main flow reverses, the vortices are ejected and trapped in the centre of the channel as the main flow passes between the wall and the vortices. If ϕ is increased to $\frac{1}{12}\pi$, as shown in figure 5(*b*), at peak flow only small asymmetry has been introduced, and the vortices appear almost unaffected. Main-flow reversal now results in ejection of

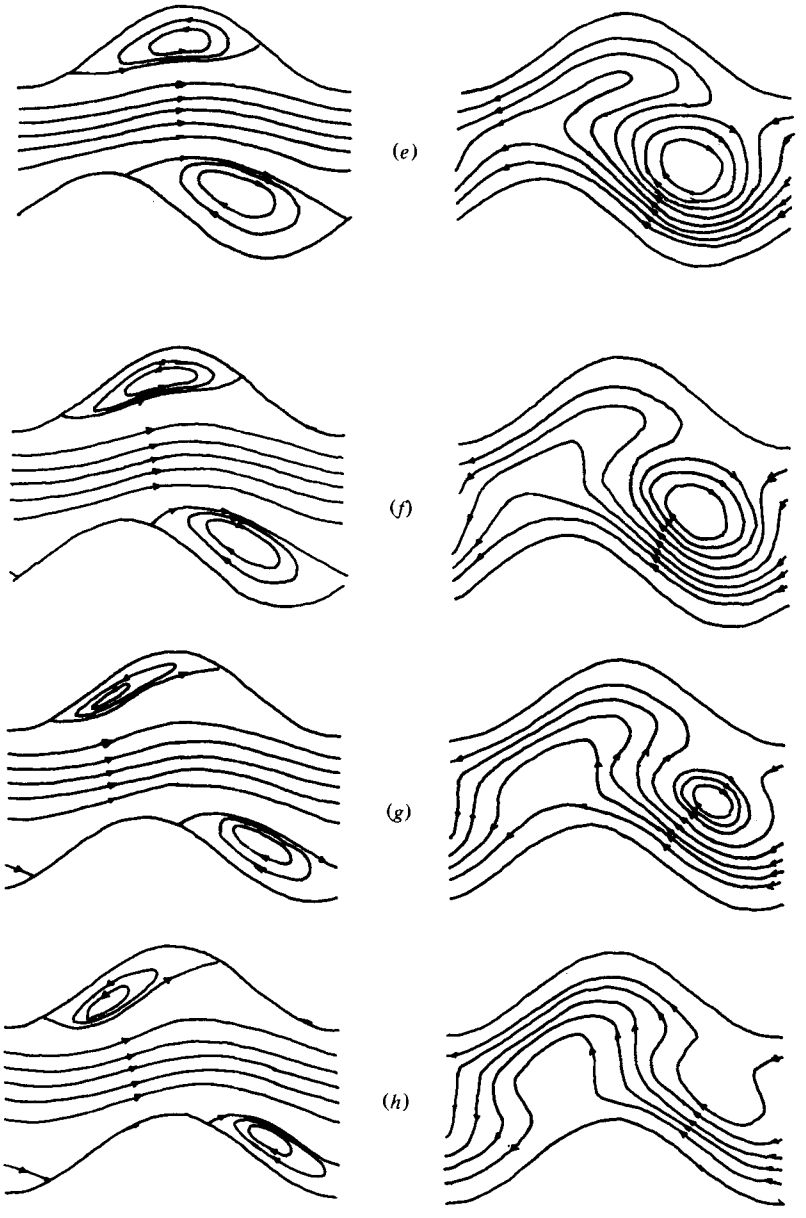

FIGURE 5. Streamlines at peak flow ($t = 0{\cdot}25$) and just after main-flow reversal ($t = 0{\cdot}52$) as the phase of the furrow asymmetry is measured; $R = 50$, $S = 0{\cdot}01$, $L = 8$, $D = 2$. (*a*) $\phi = 0$; (*b*) $\frac{1}{12}\pi$; (*c*) $\frac{1}{6}\pi$; (*d*) $\frac{1}{4}\pi$; (*e*) $\frac{1}{2}\pi$; (*f*) $\frac{2}{3}\pi$; (*g*) $\frac{5}{6}\pi$; (*h*) π.

the vortices, but now the vortices are of unequal strength, with the lower vortex the stronger. This means that some fluid passes between the two vortices as well as between the vortices and the walls. This is obviously the start of the convoluted path observed in figure 3(*d*). The vortex centres also appear to have rotated relative to each other. If ϕ increases to $\frac{1}{6}\pi$ and $\frac{1}{4}\pi$ these effects are accentuated (figures 5*c*, *d*). More fluid passes between the vortices on ejection, and the vortex in the lower furrow dominates the vortex from the upper furrow. This is also apparent from the

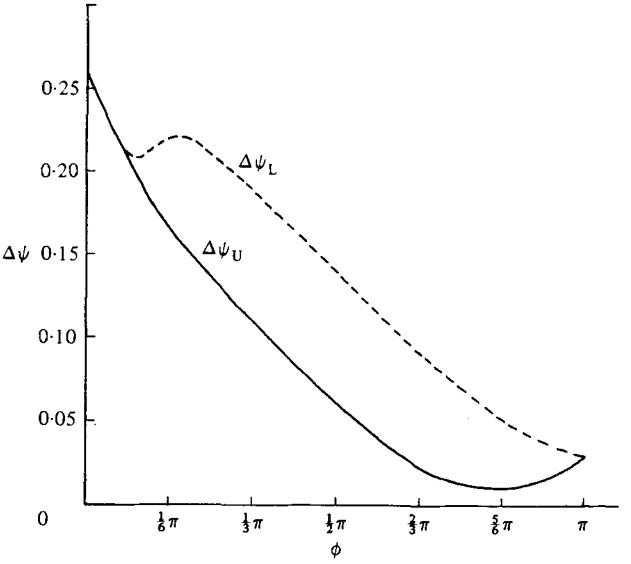

FIGURE 6. Variation of vortex strength at peak flow ($t = 0{\cdot}25$) as phase of furrow varies; $R = 50$, $S = 0{\cdot}01, L = 8, D = 2$. $\Delta\psi_L$ = vortex strength on lower wall; $\Delta\psi_U$ = vortex strength on upper wall.

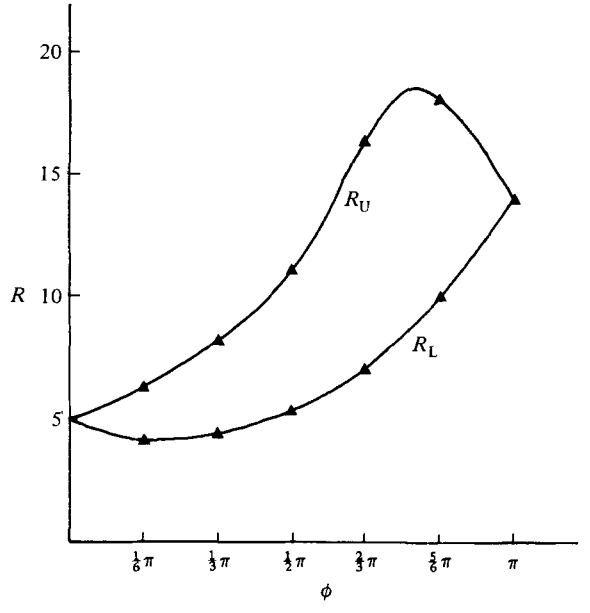

FIGURE 7. The critical Reynolds number for steady separation; $L = 8$, $D = 2$. R_L = Reynolds number on the lower wall; R_U = Reynolds number on the upper wall.

streamlines at peak flow, where considerable asymmetries in the vortex position and sizes are seen. Continued increase in ϕ results in another effect, namely the strengths of both vortices decrease, and, although the lower vortex dominates the upper one, its strength is decreasing, and eventually when $\phi = \pi$ some form of symmetry has been restored as both vortices are again of equal strength.

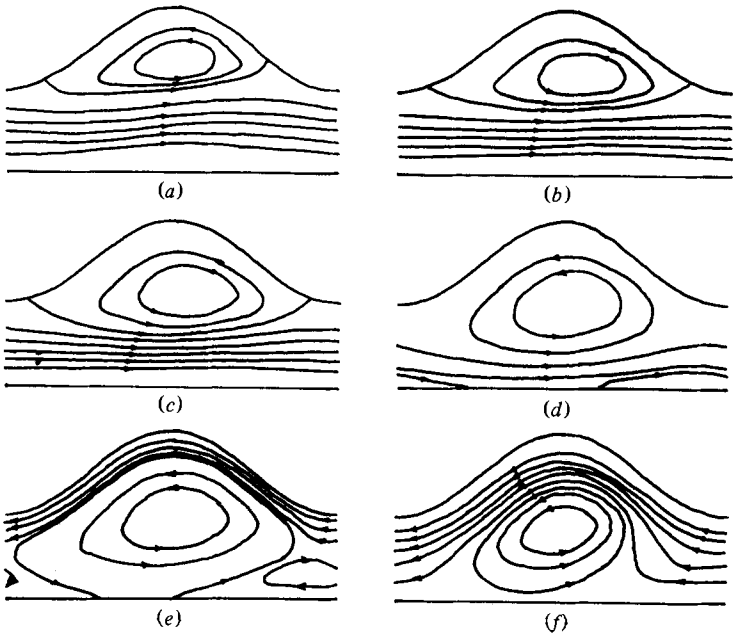

FIGURE 8. Streamlines for flow through a channel with one wall flat; $R = 50, S = 0{\cdot}01, L = 8, D = 2$. (*a*) $t = 0{\cdot}25$; (*b*) 0·4; (*c*) 0·45; (*d*) 0·495; (*e*) 0·505; (*f*) 0·52.

The strengths of the two vortices at peak flow are illustrated in figure 6. It can be seen that, if ϕ is a little larger than zero, both vortices are slightly weakened, but at a value of ϕ near $\frac{1}{12}\pi$ the upper vortex becomes much weaker than the lower one, and remains so until $\phi = \pi$. This also agrees with our intuition that the vortex strengths should be related to the rate of change of width of the channel as this is greater for the lower furrow.

We have also calculated the critical Reynolds number for separation of a steady flow in this type of channel. The results are shown in figure 7. It should be emphasized that the critical Reynolds number is a function of the furrow depth and length, so that $R_c = R_c(L, D, \phi)$ and figure 7 only shows the variation of R_c as ϕ changes from 0 to π. At both $\phi = 0$ and $\phi = \pi$ the critical Reynolds number must separate into two curves, one for the upper furrow and one for the lower. It is also important to note that if $\pi < \phi < 2\pi$ the furrows reverse, and during the time of reverse main flow, i.e. $0{\cdot}5 < t < 1$, the furrows will also be reversed.

As can be seen from figure 7 there is considerable increase in the critical Reynolds number as ϕ nears π, and the maximum value is almost four times that for a symmetric channel. This implies that to achieve a given level of mixing using oscillatory flow the Reynolds number would need to be higher in an asymmetric channel than in a symmetric channel.

5. Other geometries

In this section we look at several other geometries, the most important being a sinusoidal wall opposite a flat wall. In this case only one vortex forms, in the furrow on the sinuous wall. The basic flow cycle is illustrated in figure 8, which gives calculated streamlines for $R = 50$ and $S = 0{\cdot}01$. We have also calculated streamlines

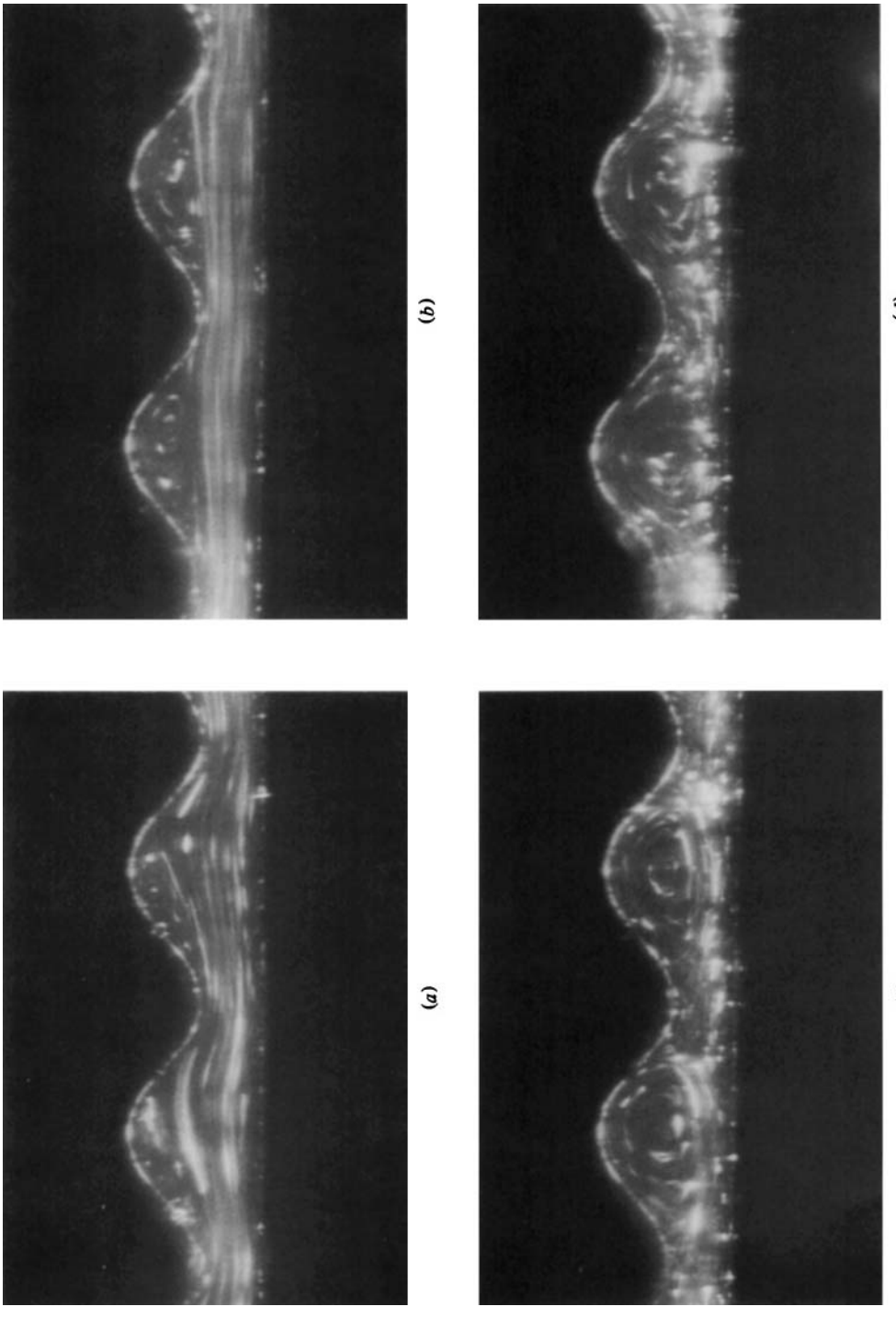

FIGURE 9. Oscillatory flow in a channel with a flat wall; $h = 1$ mm, $Lh = 4$ mm, $Re = 100$, $St = 0{\cdot}006$, flow initially from left to right. (*a*) Early in the acceleration; (*b*) near peak flow; (*c*) late in the deceleration, showing vortex expansion; (*d*) just after flow reversal, showing vortex ejection.

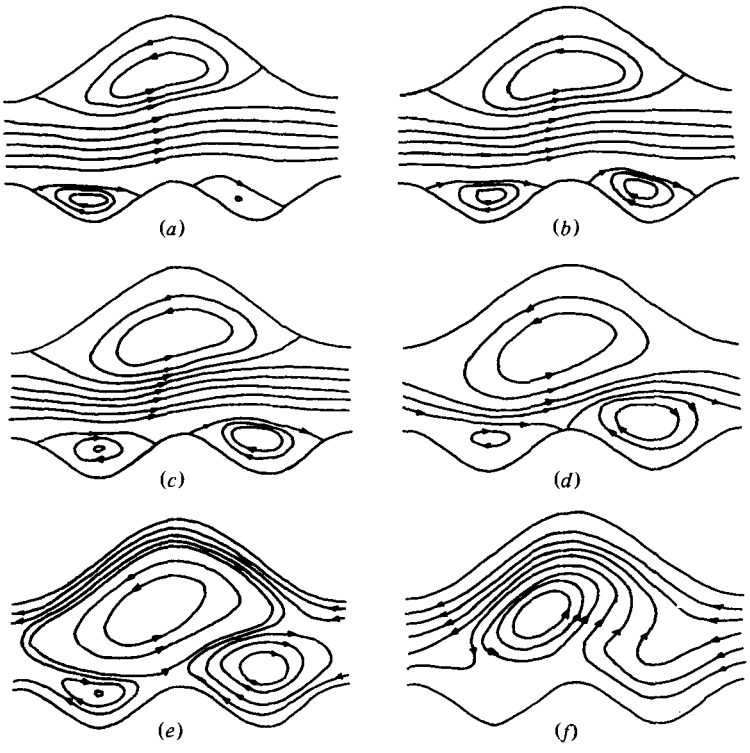

FIGURE 10. Flow in one furrow opposite two smaller furrows; $R = 50, S = 0{\cdot}01, L = 8, D = 2$ (upper wall); $L = 4$, $D = 1$ (lower wall). (*a*) $t = 0{\cdot}25$; (*b*) 0·40; (*c*) 0·45; (*d*) 0·495; (*e*) 0·505; (*f*) 0·52.

at $R = 100$, and they are essentially similar. During the acceleration the flow separates on the upper wall and a vortex forms, growing during the remainder of the flow acceleration and continuing to expand as the flow decelerates. However, during the deceleration the flow separates on the flat plate nearly opposite the downstream end of the furrow on the upper wall. Our calculations show that the strength of the lower separated region is small, indicating that its formation is due mainly to viscous action, i.e. that locally the reverse flow is similar to the reverse flow that would occur in a Stokes layer. Further evidence of this comes when the main flow reverses direction. The vortex from the upper furrow is ejected and moves to become attached to the lower wall. However, the separated region on the lower wall does not appear to be displaced (figure 8*e*), but in our calculations remains essentially a stagnant area. Further increase in the mainstream flux eliminates this region and leaves only the ejected vortex from the upper furrow (figure 8*f*). We have also photographed oscillatory flow in this type of geometry, and in figure 9 we show observations that confirm the flow patterns described above.

We have calculated the critical Reynolds number for the geometry of figure 8 to be $R_c = 8$, and this indicates that the flat wall acts as we would expect; by reducing adverse pressure gradients due to changes in channel width, the onset of separation is delayed.

Two other geometries that are interesting have two and three furrows opposite one large furrow. It is not obvious how the formation and interaction of vortices on the lower wall will occur. As can be seen from figures 10 and 11 a surprising feature emerges. As the flow accelerates, the fluid separates on the upper wall as well as in

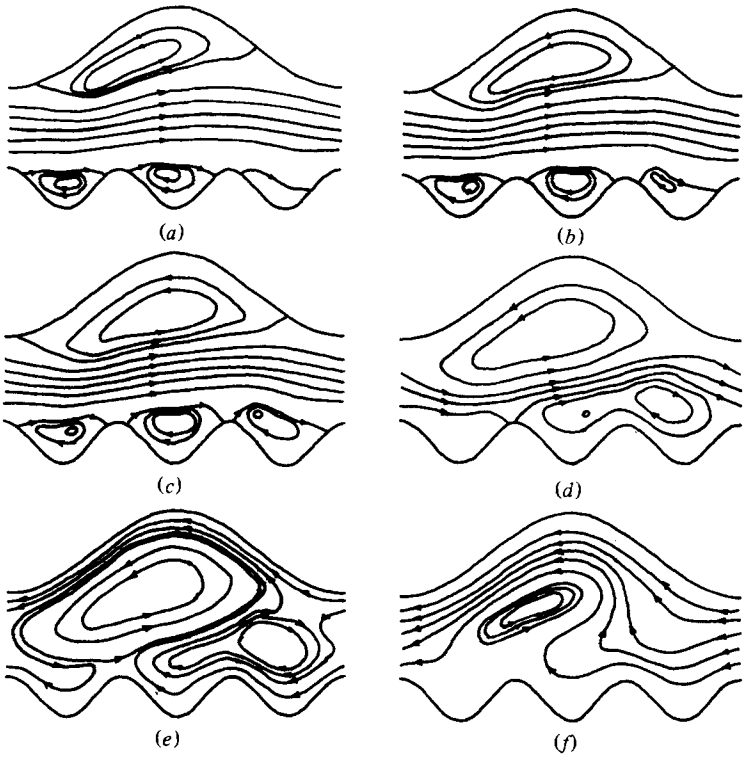

FIGURE 11. Flow in one furrow opposite three furrows; $R = 50$, $S = 0{\cdot}01$, $L = 8$, $D = 2$ (upper wall); $L = \frac{8}{3}$, $D = 1$ (lower wall). (*a*) $t = 0{\cdot}25$; (*b*) 0·4; (*c*) 0·45; (*d*) 0·495; (*e*) 0·505; (*f*) 0·52.

each of the lower furrows, although separation on the lower wall occurs first in the upstream furrow, but it is the downstream furrow that eventually dominates the lower wall. This can only be because the first vortex forms when the mainstream is relatively weak and its subsequent development is largely due to viscous diffusion of vorticity across the dividing streamline, while the second (and third) form when the mainstream flow is stronger, and thus have more energy available. In effect they obtain a greater initial kick because the main flow is greater.

6. Conclusions

We have presented the results of numerical calculations and observations of oscillatory flows in asymmetric channels when separation occurs and when the Strouhal number has an intermediate value. The most-striking feature of intermediate Strouhal number flows is the growth of the size of vortices during a deceleration. We have shown that this property exists in asymmetric geometries and have explored some of the flows that can result. Since our results are mainly numerical they lack a cohesive theory, but we believe that an unsteady flow about an arbitrary geometry will develop in a manner that can be predicted from the patterns we have shown. As an adequate description of steady separated flows is only just emerging in the literature, future work may well provide a sound theoretical description of unsteady separation. We hope that these calculated flows will act as a challenge in the development of a rational asymptotic theory of unsteady separation.

This work was supported by the S.R.C. and carried out in the Department of Engineering Science, University of Oxford.

REFERENCES

SMITH, F. T. 1976 *Q. J. Mech. Appl. Math.* **29**, 365–376.

SOBEY, I. J. 1980 *J. Fluid Mech.* **96**, 1–26.

SOBEY, I. J. 1982 Submitted to *J. Fluid Mech.*

STEPHANOFF, K., SOBEY, I. J. & BELLHOUSE, B. J. 1980 *J. Fluid Mech.* **96**, 27–32.